Overexpression of TCL1 activates the endoplasmic reticulum stress response: a novel mechanism of leukemic progression in mice

Crystina L. Kriss,[1] Javier A. Pinilla-Ibarz,[1,2] Adam W. Mailloux,[1] John J. Powers,[1] Chih-Hang Anthony Tang,[1] Chang Won Kang,[3] Nicola Zanesi,[4] Pearlie K. Epling-Burnette,[1] Eduardo M. Sotomayor,[1,2] Carlo M. Croce,[4] Juan R. Del Valle,[3] and Chih-Chi Andrew Hu[1]

[1]Department of Immunology, H. Lee Moffitt Cancer Center & Research Institute, Tampa, FL; [2]Department of Malignant Hematology, H. Lee Moffitt Cancer Center & Research Institute, Tampa, FL; [3]Drug Discovery Department, H. Lee Moffitt Cancer Center & Research Institute, Tampa, FL; and [4]Department of Molecular Virology, Immunology and Medical Genetics, The Ohio State University School of Medicine, Columbus, OH

Chronic lymphocytic leukemia (CLL) represents 30% of adult leukemia. TCL1 is expressed in ~ 90% of human CLL. Transgenic expression of TCL1 in murine B cells (Eμ-TCL1) results in mouse CLL. Here we show for the first time that the previously unexplored endoplasmic reticulum (ER) stress response is aberrantly activated in Eμ-TCL1 mouse and human CLL. This includes activation of the IRE-1/XBP-1 pathway and the transcriptionally up-regulated expression of Derlin-1, Derlin-2, BiP, GRP94, and PDI. TCL1 associates with the XBP-1 transcription factor, and causes the dysregulated expression of the transcription factors, Pax5, IRF4, and Blimp-1, and of the activation-induced cytidine deaminase. In addition, TCL1-overexpressing CLL cells manufacture a distinctly different BCR, as we detected increased expression of membrane-bound IgM and altered N-linked glycosylation of Igα and Igβ, which account for the hyperactive BCR in malignant CLL. To demonstrate that the ER stress-response pathway is a novel molecular target for the treatment of CLL, we blocked the IRE-1/XBP-1 pathway using a novel inhibitor, and observed apoptosis and significantly stalled growth of CLL cells in vitro and in mice. These studies reveal an important role of TCL1 in activating the ER stress response in support for malignant progression of CLL. (*Blood*. 2012;120(5):1027-1038)

Introduction

Chronic lymphocytic leukemia (CLL) represents 30% of adult leukemia and is an incurable B-cell malignancy. Malignant CLL cells use a limited repertoire of immunoglobulin heavy and light chain genes to manufacture their BCRs,[1-3] and are very responsive to in vitro anti-IgM stimulation.[4,5] Thus, Ag stimulation has been proposed to drive malignant progression of CLL.

The functions of the endoplasmic reticulum (ER) and its associated molecules in CLL have not attracted extensive investigative efforts because CLL cells do not exhibit a readily prominent ER structure like professional secretory cells. Although no protein Ag has been shown to drive malignant progression of CLL in vivo, exposure to Toll-like receptor ligands activates CLL cells, allowing rapid proliferation,[6,7] a cellular process accompanied by robust production and folding of membrane receptors and secretory proteins in the ER. We hypothesize that the ER may play an important role in malignant progression of CLL. First, electron microscopy examinations of human CLL cells showed clear ER expansions and immunoglobulin staining in the ER.[8-10] Second, treatments that target ER-Golgi protein transport or inhibit BiP (HSP70 in the ER) and GRP94 (HSP90 in the ER) can sensitize CLL cells to drug-induced apoptosis.[9,11,12]

The IRE-1/XBP-1 pathway is activated in response to stress conditions like proteotoxicity or hypoxia in the ER, but it also plays important roles in maintaining basal cellular functions.[13,14] IRE-1 is an ER-resident transmembrane protein that contains a stress sensor domain in the lumen of the ER, and a serine/threonine kinase domain linked to an RNase domain in the cytoplasm. On stress conditions, IRE-1 oligomerizes via its luminal domains in the ER, bringing together the cytoplasmic kinase domains which can undergo autophosphorylation and up-regulate IRE-1's RNase activity. The IRE-1 RNase then splices 26 nucleotides from the mature XBP-1 mRNA, allowing the spliced XBP-1 mRNA to encode the functional 54-kDa transcription factor XBP-1.[15-17] XBP-1 regulates a panel of important genes[18] and can crosstalk with other B-cell transcription factors, such as IRF4 and Blimp-1.[19] Overexpression of XBP-1 in B cells has been shown to cause monoclonal gammopathy of undetermined significance, a precursor condition for multiple myeloma.[20]

Here, we investigate the roles of the ER stress response in the Eμ-TCL1 CLL mouse model, in which the TCL1 gene is under the control of the immunoglobulin heavy chain promoter/enhancer driving TCL1 overexpression in B cells.[21] TCL1 is expressed in ~ 90% human CLL patients,[22] and its overexpression is associated with strong BCR signaling,[23,24] allowing malignant CLL cells to undergo high-rate proliferation. Eμ-TCL1 mice initially develop a preleukemic state with clear $CD5^+IgM^+$ B-cell characteristics in the blood, spleen, lymph nodes, and bone marrow, and slowly progress to the full-blown monoclonal CLL stage with all clinical features of aggressive human CLL.[21,25] Similar to human patients with aggressive CLL, Eμ-TCL1 mice initially respond to fludarabine (a purine analog that inhibits DNA synthesis), but quickly develop resistance and eventually die from leukemia.[26] These

Submitted November 22, 2011; accepted June 2, 2012. Prepublished online as *Blood* First Edition paper, June 12, 2012; DOI 10.1182/blood-2011-11-394346.

The online version of this article contains a data supplement.

The publication costs of this article were defrayed in part by page charge payment. Therefore, and solely to indicate this fact, this article is hereby marked "advertisement" in accordance with 18 USC section 1734.

features prompted us to use Eμ-TCL1 CLL cells to study the contribution of the ER stress response to malignant progression of CLL.

Methods

Mice

Eμ-TCL1[21] and $\mu S^{-/-}$[27] mice were maintained at our animal facility abiding by the guidelines provided by the University of South Florida and the H. Lee Moffitt Cancer Center Committees on Animal Care.

Immunofluorescent staining and flow cytometric analysis of mouse PBMCs

Peripheral blood mononuclear cells (PBMCs) were nonlethally obtained from mice after the submandibular bleed and RBC lysis (QIAGEN). Nonspecific staining was first blocked for 30 minutes at 4°C with 300 μL of FBS per 1.0×10^6 cells. Cell-surface staining was accomplished by 30-minute incubation at 4°C with 1 μL per 1.0×10^6 cells of the following anti–mouse Abs: B220–Alexa 488, CD19-allophycocyanin-Cy7 (BD Pharmingen), IgM–Alexa 568 (Invitrogen), CD5-allophycocyanin (eBioscience), and CD138-PE (BD Pharmingen). Viability staining was accomplished using 4′,6-diamidino-2-phenylindole (DAPI) exclusion (10 μg/mL; 200 μL/1×10^6 cells) during acquisition. Apoptotic cells were detected by annexin V–PE staining (BD Pharmingen). Acquisition of B-cell and CLL cell populations was performed on a LSRII cytometer (BD Biosciences) harboring a custom configuration for the H. Lee Moffitt Cancer Center & Research Institute. Mid-range Spherotech FL1 fluorescent rainbow beads (BD Biosciences) were used to maintain consistent gains for all parameters across time points. Analysis of cytometry data was achieved using FlowJo software (Version 7.6.1; TreeStar Inc).

Abs and reagents

Polyclonal Abs against Igα, Igβ, Derlin-1, Derlin-2, BiP, class I MHC, and protein disulfide isomerase (PDI) were generated in rabbits. Abs to TCL1 (Cell Signaling Technology), IRE-1 (Cell Signaling Technology), XBP-1 (Santa Cruz), Blimp-1 (Santa Cruz), IRF4 (Cell Signaling Technology), Pax5 (Santa Cruz), Syk (Cell Signaling Technology), phospho-Syk (Tyr525/526; Cell Signaling Technology), AKT (Cell Signaling Technology), phospho-AKT (Ser473; Invitrogen), ERK1/2 (Cell Signaling Technology), phospho-ERK1/2 (Thr202/Tyr204; Cell Signaling Technology), GRP94 (Stressgen), calreticulin (Stressgen), calnexin (Stressgen), phospho-eIF2α (Ser51; Cell Signaling Technology), eIF2α (Cell Signaling Technology), HSP70 (Stressgen), p97 (Fitzgerald), CHOP (Cell Signaling Technology), actin (Sigma-Aldrich), activation-induced cytidine deaminase (AID; Cell Signaling Technology), phospho-Igα (Tyr182; Cell Signaling Technology), μ (SouthernBiotech), and κ (SouthernBiotech) were obtained commercially. LPS and fludarabine were procured from Sigma-Aldrich. Tunicamycin and thapsigargin were purchased from Enzo Life Sciences.

Cell culture

B lymphocytes, $\mu S^{-/-}$ B cells, and Eμ-TCL1 CLL cells were purified from mouse spleens by negative selection using anti-CD43 magnetic beads (Miltenyi Biotec). Primary human CLL cells were obtained from consented patients at the Moffitt Cancer Center by J.A.P.-I. following the guidelines of the institutional review board in accordance with the Declaration of Helsinki. These cells as well as the 3 human CLL cell lines, MEC1, MEC2 and WaC3, and 1 mouse multiple myeloma cell line, 5TGM1, were all cultured in the RPMI 1640 media (Invitrogen) supplemented with 10% heat-inactivated fetal bovine serum (FBS), 2mM L-glutamine, 100 U/mL penicillin G sodium, 100 μg/mL streptomycin sulfate, 1mM sodium pyruvate, 0.1mM nonessential amino acids, and 0.1mM β-mercaptoethanol (β-ME).

Protein isolation and immunoblotting

Cells were lysed in radioimmunoprecipitation assay (RIPA) buffer supplemented with protease inhibitor cocktail (Roche). The protein concentrations of the supernatants were determined by BCA assay (Pierce). Samples were boiled in SDS-PAGE sample buffer with β-ME and separated by SDS-PAGE. Proteins were transferred to nitrocellulose membranes, blocked in 5% milk, and immunoblotted with the indicated Abs and appropriate horseradish peroxidase–conjugated secondary Abs. After multiple washes in PBS, the blots were developed using Western Lighting Chemiluminescence Reagent (PerkinElmer).

Reverse transcription and polymerase chain reaction

Total RNA was isolated using TRIzol reagent (Invitrogen). Complementary DNA was synthesized from RNA using Superscript II reverse transcriptase (Invitrogen). The following sets of primers were used together with Platinum Taq DNA polymerase (Invitrogen) in polymerase chain reaction (PCR) to detect the expression of: human XBP-1 (GAGTTAAGACAGCGCTTGGG and ACTGGGTCCAAGTTGTCCAG); human GAPDH (GGATGATGTTCTGGAGAGCC and CATCACCATCTTCCAGGAGC); human actin (CTGAGCGTGGCTACTCCTTC and GGCATACAGGTCCTTCCTGA); mouse XBP-1 (GATCCTGACGAGGTTCCAGA and ACAGGGTCCAACTTGTCCAG); and mouse actin (AGCCATGTACGTAGCCATCC and CTCTCAGCTGTGGTGGTGAA).

BCR activation and phosphorylation assay

Wild-type mouse B cells and Eμ-TCL1 CLL cells were suspended in RPMI 1640 serum-free media supplemented with 25mM Hepes, stimulated with $F(ab')_2$ fragments of the goat anti–mouse IgM Ab (20 μg/mL; SouthernBiotech) for 2 minutes, and lysed immediately by adding ice-cold lysis buffer (50mM Tris-HCl, pH 8.0; 150mM NaCl; 1% Triton X-100; 1mM EDTA) supplemented with protease inhibitor cocktail (Roche), 4mM sodium pyrophosphate, 2mM sodium vanadate, and 10mM sodium fluoride. The lysates were analyzed by SDS-PAGE. Phosphorylated proteins of interest were detected by immunoblots using phospho-specific Abs.

Pulse-chase experiments, immunoprecipitation, protein deglycosylation, and SDS-PAGE

B cells or CLL cells were starved in methionine- and cysteine-free media containing dialyzed serum for 1 hour, then pulse-labeled with 250 μCi/mL [^{35}S]-methionine and [^{35}S]-cysteine (PerkinElmer) for 15 minutes. After labeling, cells were incubated in chase medium containing unlabeled methionine (2.5mM) and cysteine (0.5mM). At the end of each chase interval, cells were lysed in RIPA buffer containing protease inhibitors. Precleared lysates were incubated with a primary Ab and protein G-agarose beads (Sigma-Aldrich). Bead-bound proteins were eluted using glycoprotein denaturing buffer (0.5% SDS, 1% β-ME) or reducing Laemmli SDS-PAGE sample buffer. Enzymatic deglycosylation of proteins was achieved by denaturation of the immunoprecipitates in glycoprotein denaturing buffer at 95°C for 5 minutes, followed by addition of sodium citrate (pH 5.5) to a final concentration of 50mM, and incubated with Endo H (New England Biolabs) at 37°C for 2 hours. Alternatively, sodium phosphate (pH 7.5) and NP-40 were added to the denatured cell lysates to a final concentration of 50mM and 1%, respectively, and the mixture was incubated with PNGase F (New England Biolabs) at 37°C for 2 hours. Protein samples were then analyzed by SDS-PAGE followed by fluorography.

Chemical synthesis and characterization of the IRE-1 inhibitors

STF-083010 and B-A05 were synthesized in-house from commercially available reagents as described in supplemental Methods (available on the *Blood* Web site; see the Supplemental Materials link at the top of the online article). STF-083010 stability studies were performed using analytical reverse-phase high-pressure liquid chromatography (RP-HPLC) with a C_{18} column (4 mm × 150 mm) and a 10%-90% linear gradient of acetonitrile in water (containing 0.1% formic acid) as eluent more than 20 minutes (1 mL/min flow rate). Compounds were detected at $\lambda = 254$ nm. Crystalline STF-083010 was analyzed on a standard Bruker X8 Apex2 CCD-based

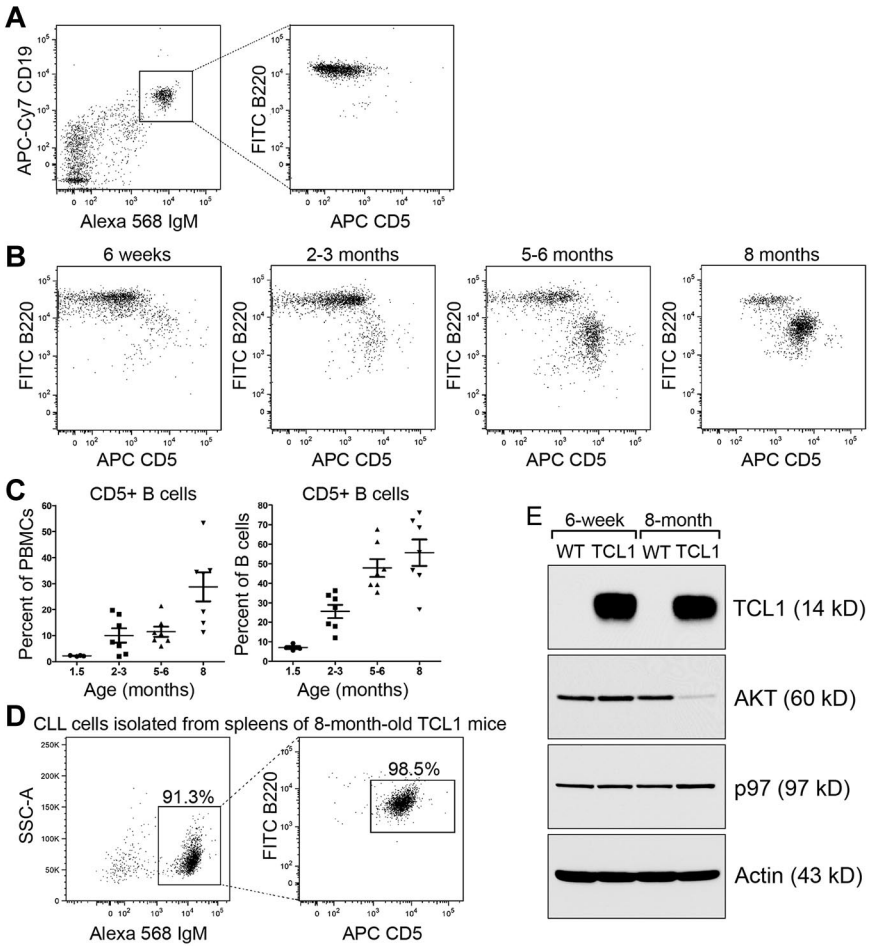

Figure 1. CLL cells purified from spleens of 8-month-old Eμ-TCL1 mice express reduced amounts of AKT. (A) PBMCs isolated from 8-month-old wild-type mice were stained with CD19-APC-Cy7, IgM-Alexa568, CD5-APC, B220–Alexa 488, and DAPI. Live PBMCs were analyzed for $CD5^+/B220^+$ CLL cells on gated $CD19^+/IgM^+$ B-cell populations. Data are representative of 3 independent experiments. (B) PBMCs isolated from Eμ-TCL1 mice of different age groups were stained with CD19-APC-Cy7, IgM–Alexa 568, CD5-APC, B220–Alexa 488, and DAPI. Live PBMCs were analyzed for $CD5^+/B220^+$ CLL cells on gated $CD19^+/IgM^+$ B-cell populations. Data are representative of more than 4 independent experiments. (C) $CD5^+/B220^+$ CLL were plotted against PBMCs or $CD19^+/IgM^+$ B cells. Each dot represents an individual mouse, and horizontal bars indicate means of at least 4 experiments. (D) IgM^+ cells purified from spleens of Eμ-TCL1 mice were analyzed for the presence of $CD5^+/B220^+$ CLL cells. Data are representative of 3 independent experiments. (E) Lysates from CD5-/$B220^+$ B cells of 6-week-old wild-type (WT) and Eμ-TCL1 mice (lanes 1 and 2), from CD5-/$B220^+$ B cells of 8-month-old wild-type mice (lane 3), and from $CD5^+/B220^+$ CLL cells of 8-month-old Eμ-TCL1 mice (lane 4) were immunoblotted for TCL1, AKT, p97, and actin. Results shown in each immunoblot are representative of 3 independent experiments. For each experiment, $CD5^-/B220^+$ B cells, $CD5^-/B220^+$ Eμ-TCL1 B cells, and $CD5^+/B220^+$ CLL cells were purified and pooled from at least 2 spleens of mice with indicated genotypes.

x-ray diffractometer, and the solid-state structure was solved and refined with the Bruker SHELXTL (Version 6.12) software package. Diffraction data (excluding structure factors) for STF-083010 have been deposited with the Cambridge Crystallographic Data Center as supplementary CCDC publication number 850879.

Cell-proliferation assays

Eμ-TCL1, MEC1, MEC2, WaC3, or primary human CLL cells were grown in 96-well cell-culture plates overnight and then treated with fresh phenol red–free culture medium containing STF-083010 (50μM), A-I06 (50μM), A-I07 (50μM), or fludarabine (30μM). Every 24th hour, cells were spun down and proliferative capabilities were assessed by XTT assays (Roche) according to the manufacturer's instructions. Briefly, 50 μL of XTT labeling reagent was combined with 1 μL of electron-coupling reagent, and the mixture was applied to each well of the 96-well plates. The test was based on cleavage of the yellow tetrazolium salt XTT by mitochondrial dehydrogenases of the metabolic active cells to form the orange formazan compound, which can be spectrophotometrically quantified at 492 nm using a BioTek microplate reader.

In vivo treatment of mouse CLL with A-I06

Older Eμ-TCL1 mice (age $>$ 8 months) with high CLL burden in the peripheral blood were identified by examining the percentage of CLL cells in PBMCs. These mice then received intraperitoneal injections with A-I06 (60 mg/kg) dissolved in Cremophor ELP (vehicle; Sigma-Aldrich). The progression of CLL was monitored by flow cytofluorometry.

Results

Prolonged TCL1 expression causes a reduced expression level of AKT

To monitor malignant progression of CLL in Eμ-TCL1 mice, we took mice of different ages (ranging from 6-weeks to 8-months old) and immunostained purified PBMCs using fluorescent Abs against mouse CD19, IgM, B220, and CD5. We analyzed $B220^+/CD5^+$ CLL cells on gated $CD19^+/IgM^+$ B-cell populations of Eμ-TCL1 mice (Figure 1A), and confirmed that increased numbers of CLL cells are positively correlated to the age of Eμ-TCL1 mice when compared with PBMCs or peripheral B cells (Figure 1B-C).[21] To purify CLL cells, we killed 8-month-old Eμ-TCL1 mice with clear CLL presentation, and purified CLL cells from spleens by staining splenocytes with CD43 MicroBeads and performing negative selection using MACS columns. We consistently obtained a cell population containing $\sim$ 90% $CD5^+$ CLL cells from spleens of 8-month-old Eμ-TCL1 mice (Figure 1D). We also performed exactly the same purification using 6-week-old Eμ-TCL1 mice, and obtained a precancerous B-cell population containing consistently $<$ 1% $CD5^+$ cells. By immunoblots, we found both precancerous Eμ-TCL1 B cells and CLL cells express abundant TCL1 proteins, encoded from the Eμ-TCL1 transgene. Although TCL1 is believed to function via AKT to promote CLL formation,[28,29] prolonged TCL1 expression leads to a decreased expression of

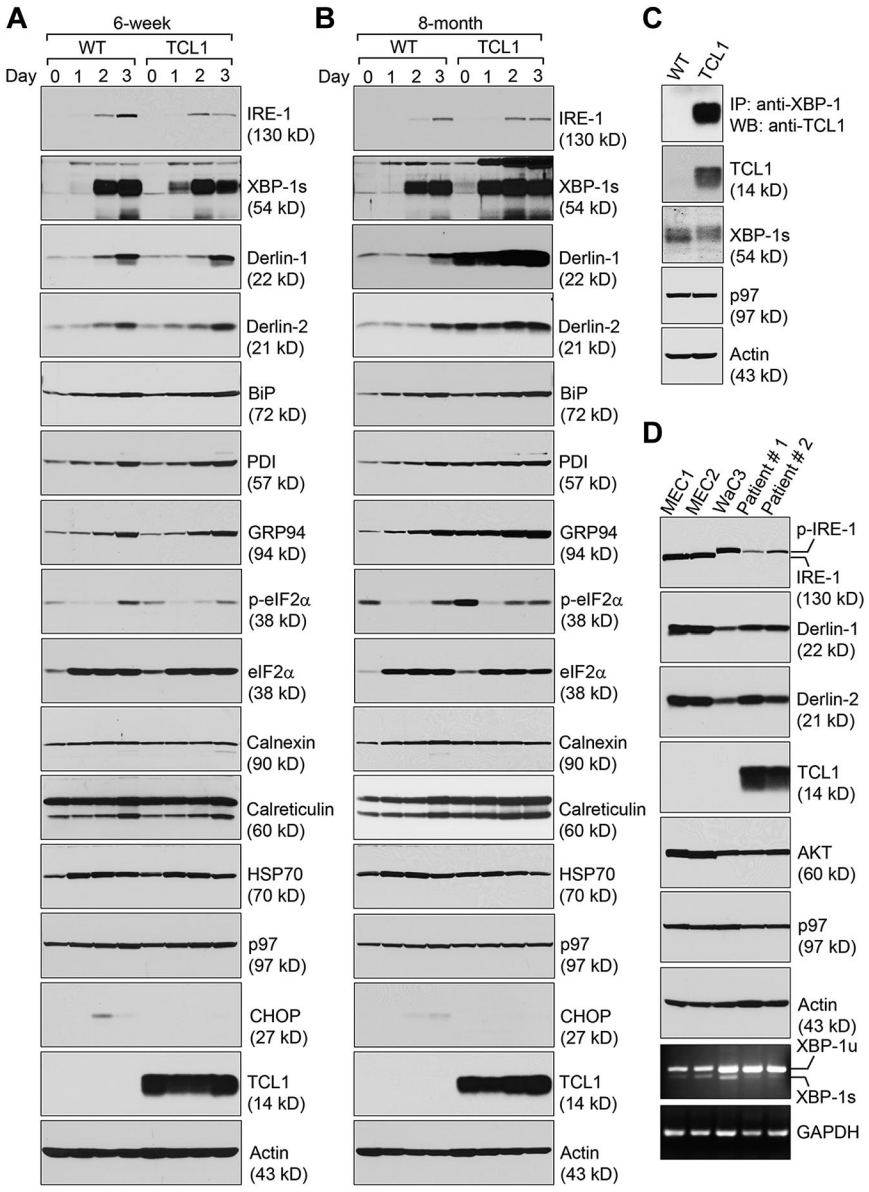

Figure 2. CLL cells express significantly increased levels of molecules involved in alleviating the ER stress. (A) CD5$^-$/B220$^+$ B cells purified from 6-week-old wild-type and Eμ-TCL1 mice were stimulated with LPS for a course of 3 days, and lysed for analysis by immunoblots for indicated proteins. Results shown in each immunoblot are representative of 3 independent experiments. For each experiment, CD5$^-$/B220$^+$ wild-type and Eμ-TCL1 B cells were purified and pooled from at least 2 mouse spleens. (B) CD5$^-$/B220$^+$ B cells purified from 8-month-old wild-type mice and CD5$^+$/B220$^+$ CLL cells from 8-month-old Eμ-TCL1 mice were stimulated by LPS for 3 days and lysed for analysis by immunoblots for indicated proteins. Results shown in each immunoblot are representative of 3 independent experiments. For each experiment, CD5$^-$/B220$^+$ wild-type B cells and CD5$^+$/B220$^+$ CLL cells were purified and pooled from at least 2 mouse spleens. (C) Association of TCL1 with XBP-1. CD5$^-$/B220$^+$ B cells purified from 8-month-old wild-type mice and CD5$^+$/B220$^+$ CLL cells from 8-month-old Eμ-TCL1 mice were stimulated by LPS for 3 days and lysed for analysis by immunoblots for TCL1, XBP-1, p97, and actin. The anti-XBP-1 Ab was used to perform immunoprecipitations from the same lysates, and the immunoprecipitates were analyzed for the presence of TCL1 (top panel). Results shown in each immunoblot are representative of 3 independent experiments. For each experiment, CD5$^-$/B220$^+$ wild-type B cells and CD5$^+$/B220$^+$ CLL cells were purified and pooled from at least 2 mouse spleens. (D) Human CLL cell lines (MEC1, MEC2, and WaC3) and freshly purified primary human CLL cells from 2 clinical patients (patient 1 and patient 2) were analyzed by immunoblots for the expression of indicated proteins. Unspliced and spliced forms of human XBP-1 mRNA (XBP-1u and XBP-1s, respectively), and human GAPDH mRNA were detected by reverse transcription followed by PCR using specific primers. Results are representative of 3 independent experiments.

AKT (Figure 1E), suggesting that TCL1 may also contribute to malignant progression of CLL by other mechanisms. Control experiments showed no changes in the expression of the Syk or ERK kinase (supplemental Figure 1).

Prolonged TCL1 expression leads to up-regulated levels of the ER stress-response molecules

Because of the lack of suitable protein Ag to stimulate polyclonal Eμ-TCL1 CLL cells in vitro, we examined the expression of ER stress-response molecules in CD5$^-$ precancerous and CD5$^+$ cancerous Eμ-TCL1 B cells stimulated with lipopolysaccharides (LPS) for a course of 3 days. We investigated the expression of IRE-1, XBP-1, Derlin proteins, BiP, GRP94, PDI (which catalyzes disulfide formation), eukaryotic initiation factor 2α (eIF2α; whose phosphorylation inhibits protein synthesis to relieve ER stress), calnexin and calreticulin, all of which are ER stress-response molecules. We found that the expression pattern of most ER proteins in precancerous Eμ-TCL1 B cells from 6-week-old mice is comparable with that of B cells purified from age-matched wild-type mice. One exception is the early onset of XBP-1 protein expression in precancerous Eμ-TCL1 B cells as a response to LPS stimulation (Figure 2A). We then compared Eμ-TCL1 CLL cells from 8-month-old mice with normal B cells from age-matched wild-type mice. Even before LPS stimulation, Eμ-TCL1 CLL cells already expressed XBP-1, Derlin-1, Derlin-2, BiP, GRP94, PDI, and phospho-eIF2α at significantly higher levels than their wild-type counterparts (Figure 2B). Stimulation with LPS allows us to detect striking differences in the expression of IRE-1, XBP-1, Derlin-1, and Derlin-2 (Figure 2B). Little change in the expression of eIF2α, calnexin, and calreticulin was observed even when Eμ-TCL1 CLL cells were stimulated with LPS. We did not detect any difference in the expression of p97 (also known as AAA-ATPase) and HSP70 in the cytoplasm (Figure 2B). While some wild-type B cells expressed the C/EBP-homologous protein (CHOP; which mediates apoptosis during ER stress) after cultured in LPS for 2 days, precancerous Eμ-TCL1 B cells and Eμ-TCL1 CLL cells did not express CHOP (Figure 2A-B). All of these data support that Eμ-TCL1 CLL cells respond to LPS by up-regulating

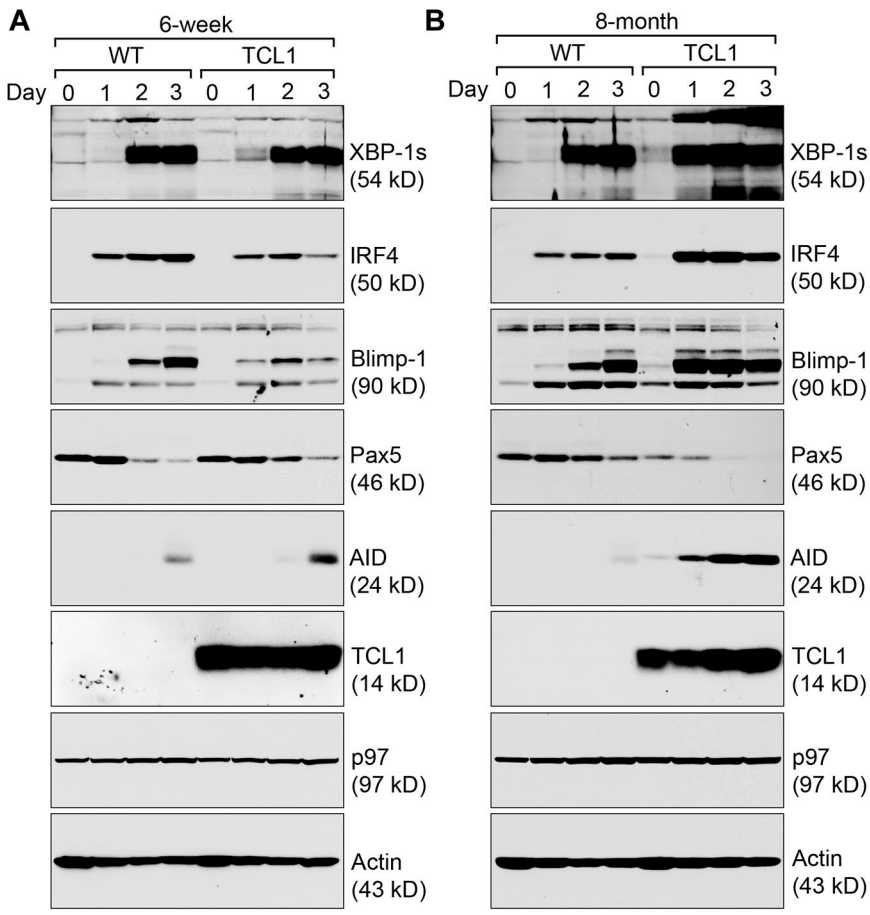

Figure 3. Eμ-TCL1 CLL cells express XBP-1, IRF4, Blimp-1, and AID at higher levels. (A) $CD5^-/B220^+$ B cells purified from 6-week-old wild-type and Eμ-TCL1 mice were stimulated with LPS for a course of 3 days, and lysed for analysis by immunoblots for indicated proteins. Data shown in each immunoblot are representative of 3 independent experiments. For each experiment, $CD5^-/B220^+$ wild-type and Eμ-TCL1 B cells were purified and pooled from at least 2 mouse spleens. (B) $CD5^-/B220^+$ B cells purified from 8-month-old wild-type mice and $CD5^+/B220^+$ CLL cells from 8-month-old Eμ-TCL1 mice were stimulated by LPS for 3 days and lysed for analysis by immunoblots for indicated proteins. Data shown in each immunoblot are representative of 3 independent experiments. For each experiment, $CD5^-/B220^+$ wild-type B cells and $CD5^+/B220^+$ CLL cells were purified and pooled from at least 2 mouse spleens.

the ER stress response to sustain robust proliferation (supplemental Figure 2A). Different from LPS, pharmacologic ER stress inducers like thapsigargin (Tg) and tunicamycin (Tu) do not promote Eμ-TCL1 CLL cell growth or elicit activation of the IRE-1/XBP-1 pathway of the ER stress response (supplemental Figure 2A-B).

To establish a link between TCL1 and activation of the ER stress response, we hypothesized that TCL1 may associate with XBP-1 to up-regulate the expression of chaperones at the transcriptional level. We discovered TCL1 in the immunoprecipitates retrieved from lysates of LPS-stimulated Eμ-TCL1 CLL cells using an anti–XBP-1 Ab (Figure 2C). The mRNA levels of total XBP-1, spliced XBP-1, Derlin-1, Derlin-2, Derlin-3, BiP, PDI, and GRP94 were all significantly elevated in LPS-stimulated Eμ-TCL1 CLL cells when compared with those in LPS-stimulated wild-type B cells (supplemental Figure 3).

To establish relevance, IRE-1, XBP-1, Derlin-1, and Derlin-2 were found expressed in human CLL cell lines (MEC1, MEC2, and WaC3) and primary CLL cells freshly isolated from 2 patients (Figure 2D), with constitutively phosphorylated IRE-1 observed in WaC3 and the 2 primary human CLL cells (Figure 2D). TCL1 is expressed in primary human CLL cells, consistent with reported observations[22] (also see "Discussion").

Overexpression of TCL1 results in dysregulated expression of B-cell transcription factors and AID

TCL1 is a transcriptional regulator, and its overexpression causes an earlier and elevated expression of XBP-1 (Figures 2A-B, 3). Because TCL1 can associate with the XBP-1 transcription factor (Figure 2C), we examined how other transcription factors crucial for B cells would respond to TCL1 overexpression as the expression of transcription factors in B cells is tightly regulated.[19] In precancerous Eμ-TCL1 B cells stimulated with LPS, we found IRF4 and Blimp-1 expressed at decreased levels, and correspondingly, a persistent expression of the transcription suppressor Pax5 (Figure 3A). Such data suggest that a dysregulated B-cell differentiation exists in precancerous Eμ-TCL1 B cells. In contrast, Eμ-TCL1 CLL cells already express Pax5 at a decreased level (Figure 3B). On stimulation by LPS, the levels of Pax5 were further reduced, possibly causing IRF4 and Blimp-1 to express at significantly increased levels (Figure 3B). To link dysregulation of transcription factors to malignant progression of CLL, we showed a dramatic increase in the expression of AID (Figure 3B), which is directly regulated by IRF4.[30] Despite significantly elevated levels of XBP-1, IRF4, Blimp-1, and AID, Eμ-TCL1 CLL cells do not acquire the $CD138^+$ immunophenotype like mouse 5TGM1 multiple myeloma cells (supplemental Figure 4).

TCL1 overexpression contributes to a constitutively active BCR, possibly because of increased expression of IgM and altered N-linked glycosylation of Igα and Igβ

The malignant features of CLL cells are manifest in their robust, constitutive BCR signaling.[31] A functional BCR consists of a membrane-bound IgM (mIgM) and a membrane-bound disulfide-linked Igα and Igβ heterodimer. Both mIgM and Igα/Igβ are manufactured and assembled in the ER, and transported through the secretory pathway via the Golgi apparatus en route to the cell surface. Because the expression of XBP-1 plays such an important role in maintaining normal BCR signaling,[19] we used $F(ab')_2$

fragments from goat anti–mouse IgM Abs to crosslink and activate the BCR of LPS-stimulated Eμ-TCL1 CLL cells, within which XBP-1 is overexpressed (Figures 2B, 3B). Strikingly different from wild-type B cells, the BCR of LPS-stimulated Eμ-TCL1 CLL cells is already conducting signal transduction even before stimulation with $F(ab')_2$ fragments, as we observed constitutive phosphorylation of Igα and the Syk kinase (Figure 4A). On stimulation with $F(ab')_2$ fragments, BCR signal transduction in Eμ-TCL1 CLL cells can be further strengthened to allow phosphorylation of 2 downstream kinases, ERK and AKT (Figure 4A). Notably, $F(ab')_2$-mediated BCR signal transduction in Eμ-TCL1 CLL cells is slightly weaker than that in wild-type B cells (Figure 4A), possibly because of less unengaged BCR available for crosslinking.

To provide an explanation for constitutive activation of the BCR, we investigated how altered levels of ER stress-response proteins may have contributed to the synthesis, assembly, and trafficking of the BCR and other integral membrane and secretory proteins in Eμ-TCL1 CLL cells. Eμ-TCL1 CLL cells express more mIgM (Figure 4B). In addition, Eμ-TCL1 CLL cells also synthesize and secrete more secretory IgM (sIgM; Figure 4B-D), as demonstrated by pulse-chase experiments in which we radiolabeled Eμ-TCL1 CLL cells, chased with cold media to allow IgM to be secreted, and retrieved radiolabeled IgM from cell lysates and culture media using an anti-μ or an anti-κ Ab (Figure 4C-D). The κ light chains recovered from Eμ-TCL1 CLL cells exhibit as a sharper band in the SDS-PAGE gel, suggesting that these CLL cells have undergone clonal selection to use a limited repertoire of κ chains for IgM assembly.

We also performed pulse-chase experiments to examine the expression and surface display of the Igα/Igβ heterodimer. Because Igβ is the limiting step for the heterodimer assembly in the ER,[19,32] we retrieved the heterodimer from Eμ-TCL1 CLL cell lysates using an anti-Igβ Ab. To reveal glycosylation status of Igα and Igβ, we treated the immunoprecipitated samples with endoglycosidase H (endo-H) to remove mannose glycans or with PNGase F to remove the entire N-linked glycans. We discovered that both Igα and Igβ in Eμ-TCL1 CLL cells are modified by distinctly different glycans when compared with those in wild-type B cells (Figure 4E). In Eμ-TCL1 CLL cells, Igβ acquires significantly more complex glycans in the Golgi apparatus (thus moving slower in the SDS-PAGE gel), but its assembled partner Igα only receives incomplete glycan modifications and thus still remains endo-H–sensitive (Figure 4E). We hypothesize that such distinct glycan modifications on Igα and Igβ may contribute to a hyperresponsive BCR in CLL cells. Such altered glycan modifications seem restricted to the BCR as they do not occur to the heavy chain (HC) of class I MHC molecules (Figure 4F). Protein transportation in the secretory pathway is clearly unaltered, as evidenced by normal secretion of sIgM and normal surface display of Igα, Igβ, and class I MHC molecules (Figure 4C-F).

A-I06, a specific inhibitor to the RNase activity of IRE-1, down-regulates the expression of XBP-1 and mimics XBP-1–deficient phenotypes in B cells

An inhibitor of IRE-1 RNase activity, STF-083010, was recently identified from a commercial screening library.[33] It shows promising effects in inhibiting proliferation of multiple myeloma without observed systemic toxicity in mice. We carried out the chemical synthesis of STF-083010 (supplemental Methods), and confirmed its structure using small-molecule x-ray diffraction (Figure 5A). While stable in crystalline form, we observed that stock solutions of STF-083010 in dimethyl sulfoxide (DMSO) readily hydrolyzed into precursors A-I06 and A-I07 after repeated freeze-thaw cycles. The instability of STF-083010 in aqueous conditions was confirmed by its complete decomposition on brief exposure to a 1:1 DMSO:water mixture (Figure 5B). We treated LPS-stimulated wild-type mouse B cells, LPS-stimulated mouse Eμ-TCL1 CLL cells, and human WaC3 CLL cells with STF-083010, A-I06, or A-I07 using various regimens, and found STF-083010 and A-I06 suppress the expression of XBP-1 (Figure 5C-D, supplemental Figure 5A), as a result of inhibiting the splicing of XBP-1 mRNA by IRE-1 (Figure 5E-F, supplemental Figure 5B,D,E). Chemical inhibition of XBP-1 by these IRE-1 inhibitors phenocopies XBP-1 deficiency introduced to B cells by gene deletion because the expression of IRE-1 is up-regulated at both protein and mRNA levels (Figure 5C, supplemental Figure 5C), and the synthesis of sIgM but not mIgM is inhibited by A-I06 (Figure 5G).[19] We then prepared a nonhydrolyzable version of STF-083010, B-A05, to test the possibility that a stabilized analog may also block IRE-1 RNase activity. In contrast to A-I06, B-A05 did not significantly alter XBP-1 expression (supplemental Figure 5G). These data establish the use of A-I06 as a specific inhibitor of the IRE-1/XBP-1 pathway and suggest that A-I06 is responsible for the presumed activity of STF-083010 (during review of this manuscript, another group reported the same finding and proposed that A-I06 forms a stable Schiff base with Lys907 in the RNase domain of IRE-1[34]).

As genetic ablation of XBP-1 does not affect secretion of sIgM and surface display of mIgM in B cells,[19] we wondered whether A-I06 would exert similar effects in B cells. To investigate the secretion of sIgM, we stimulated B cells with LPS for 2 days to allow the expression of sIgM, treated these B cells for additional 24 hours with A-I06 to inhibit the expression of XBP-1, performed pulse-chase experiments, and immunoprecipitated IgM from cell lysates and culture media using an anti-μ Ab. A-I06–treated B cells synthesize less sIgM, which can all be secreted into culture media (Figure 6A-B). Because mIgM and sIgM differ only in a short transmembrane domain, it is difficult to resolve them in the SDS-PAGE gel. To investigate the surface display of mIgM, we took advantage of $\mu S^{-/-}$ B cells, which have been genetically manipulated to allow expression of only membrane-bound μ heavy chain.[27] In similar pulse-chase experiments, we found the surface display of mIgM is not affected by treatment with A-I06, as evidenced by successful acquisition of complex glycans on the μ heavy chain (Figure 6C). The A-I06–treated $\mu S^{-/-}$ B cells also produce comparable amounts of membrane-bound μ chains and κ light chains, and the latter can be secreted into culture media (Figure 6C-D). Wild-type and $\mu S^{-/-}$ B cells also synthesize and present class I MHC molecules to their surface when treated with A-I06 (Figure 6E-F).

Down-regulated expression of XBP-1 by A-I06 leads to apoptosis of CLL cells in culture and in mice

We determined a 50% growth inhibition concentration (GI50) of ~ 50μM for human WaC3 CLL cells treated with A-I06 (supplemental Figure 6A). At 50μM concentration, A-I06 and STF-083010 exert similar growth inhibitory effects in human CLL cells (supplemental Figure 6B). When Eμ-TCL1 CLL cells were treated with STF-083010 or A-I06, we observed ~ 70% growth inhibition after 3 days (Figure 7A). Increased apoptosis was detected in Eμ-TCL1 CLL cells exposed to 50μM or 100μM A-I06 for 24 hours (supplemental Figure 7). Next, human MEC1, MEC2, and WaC3 CLL cell lines were treated with these compounds. MEC1

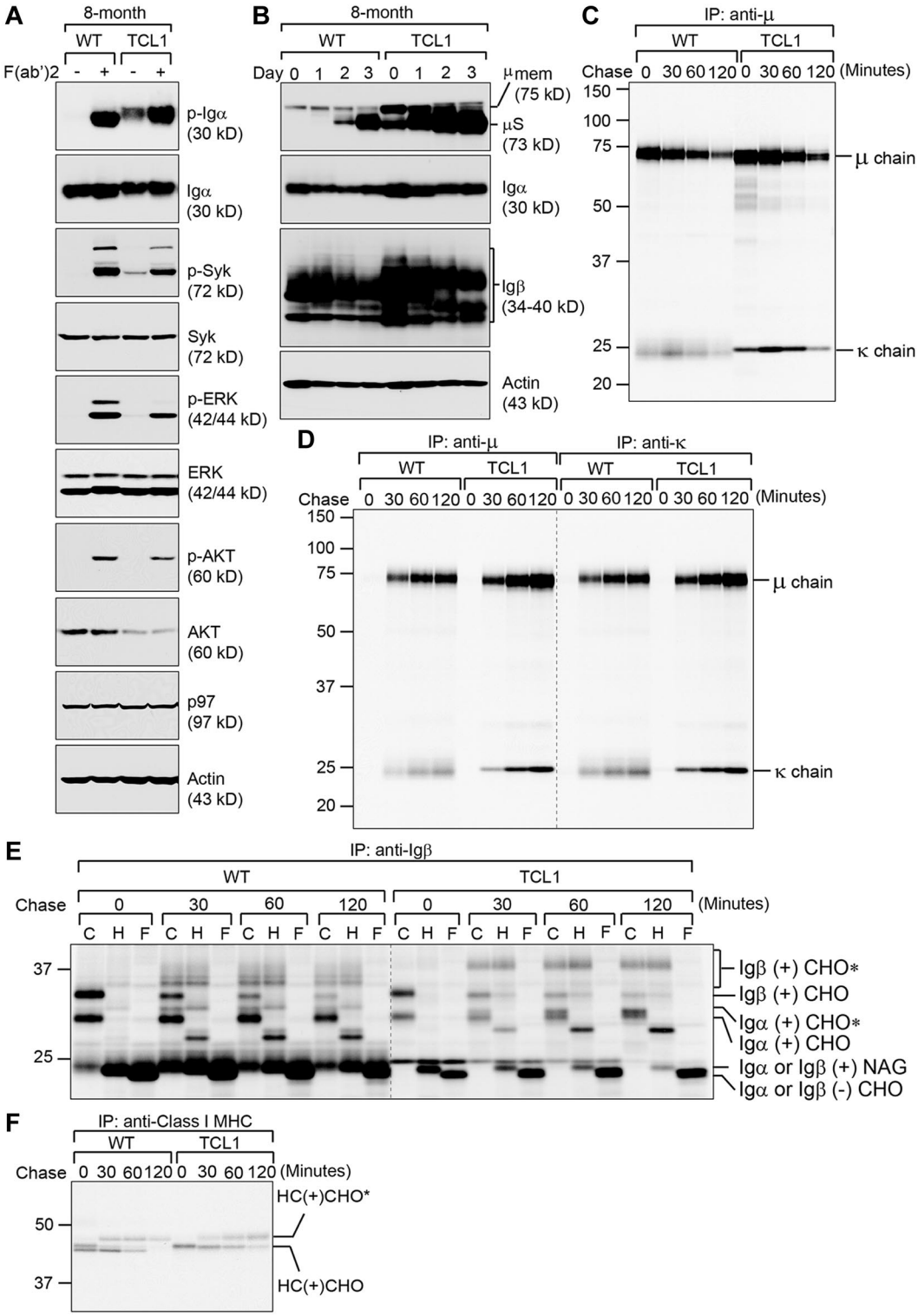

Figure 4. CLL cells from Eμ-TCL1 mice express a constitutively active BCR, which may be a result of altered glycosylation of the BCR. (A) Wild-type B cells and CLL cells isolated from 8-month-old wild-type and Eμ-TCL1 mice were cultured in the presence of LPS for 3 days. Their BCR is subsequently activated by F(ab')2 fragments of the goat anti–mouse IgM Ab for 2 minutes. Cells were immediately lysed for analysis by immunoblots using Abs against indicated molecules. Data shown in each immunoblot are representative of 3 independent experiments. For each experiment, $CD5^-/B220^+$ wild-type B cells and $CD5^+/B220^+$ Eμ-TCL1 CLL cells were purified and pooled from at least 2 mouse spleens. (B) Wild-type B cells and CLL cells isolated from 8-month-old wild-type and Eμ-TCL1 mice were stimulated with LPS for indicated days and lysed for analysis by immunoblots using Abs to immunoglobulin μ heavy chain, Igα, Igβ, and actin. Data shown in each immunoblot are representative of 3 independent experiments. For each experiment, CD5-/$B220^+$ wild-type B cells and $CD5^+/B220^+$ Eμ-TCL1 CLL cells were purified and pooled from at least 2 mouse spleens. (C) Wild-type B cells and Eμ-TCL1 CLL cells purified from 8-month-old mice were radiolabeled for 15 minutes, chased for the indicated time, and lysed. Intracellular IgM was immunoprecipitated from the lysates using an anti-μ Ab, and analyzed on an SDS-PAGE gel. Data are representative of 3 independent experiments. For each experiment, wild-type B cells and Eμ-TCL1 CLL cells were purified and pooled from 2 mouse spleens. (D) Similarly, extracellular sIgM was immunoprecipitated from culture media using an anti-μ or an anti-κ Ab and analyzed by SDS-PAGE. Data are representative of 3 independent experiments. (E) Using similar lysates as those in panel C, we performed immunoprecipitations using an anti-Igβ Ab to retrieve the Igα/Igβ heterodimers. Immunoprecipitated proteins were eluted from the beads and treated with endo-H or PNGase F before analysis by SDS-PAGE. CHO, CHO*, NAG represent high mannose-type glycans, complex-type glycans, and N-acetylglucosamines, respectively. Data are representative of 3 independent experiments. (F) Similar lysates (as panel C) were immunoprecipitated using an Ab against the class I MHC heavy chain (HC), and immunoprecipitates were analyzed by SDS-PAGE. Data are representative of 3 independent experiments.

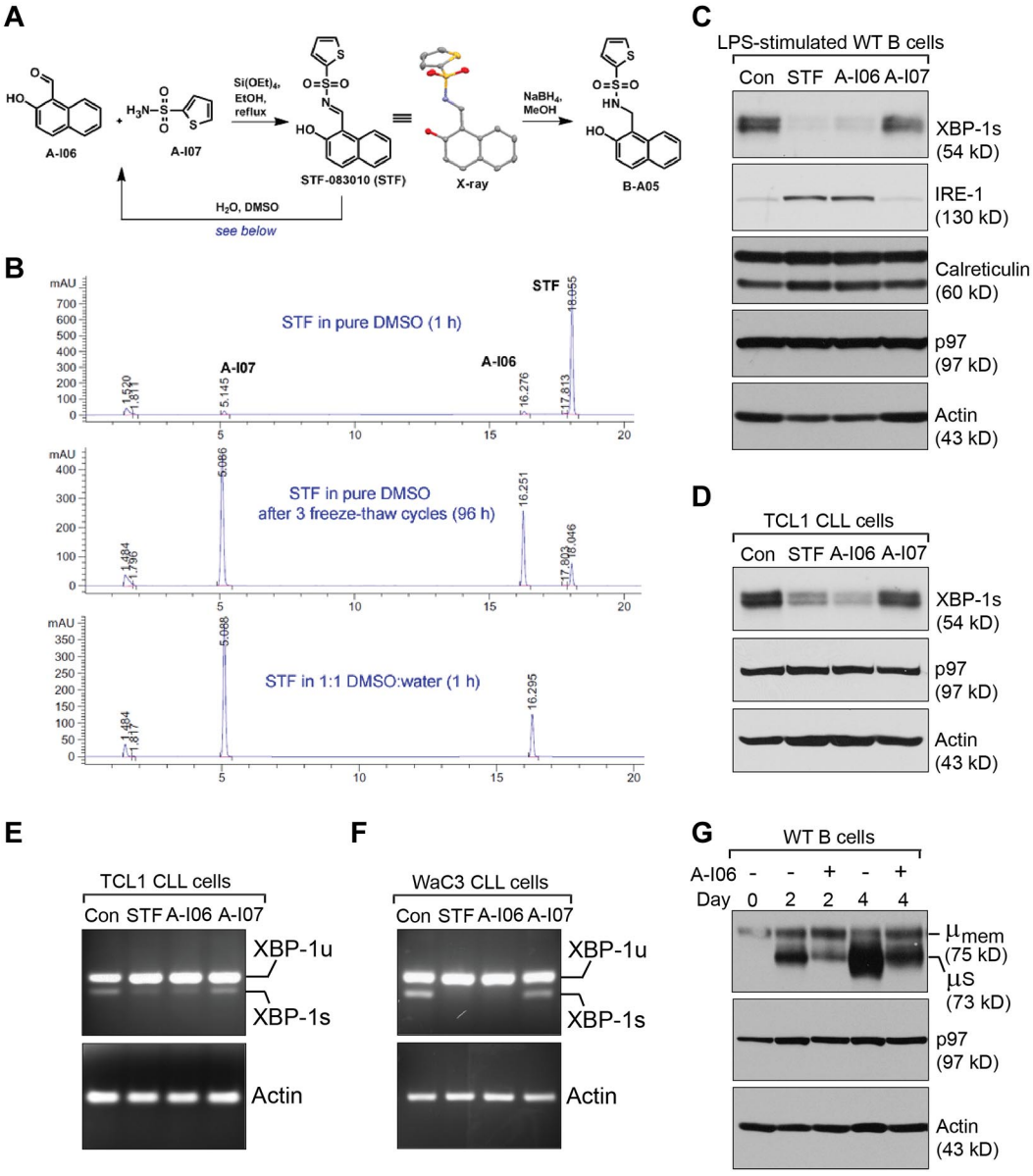

Figure 5. A-I06 suppresses the expression of functional XBP-1, and A-I06–treated B cells phenocopy B cells deleted with XBP-1 gene. (A) Structures and chemical synthesis of A-I06, A-I07, STF-083010, and B-A05, including the x-ray structure of STF-083010 with hydrogens omitted for clarity. (B) Assessment of STF-083010 aqueous stability using RP-HPLC. Injection of the freshly prepared DMSO stock solution of crystalline STF-083010 showed only minimal decomposition. STF-083010 subjected to multiple freeze-thaw cycles showed significant breakdown. Dissolution of STF-083010 in a 1:1 DMSO:water mixture resulted in complete conversion to A-I06 and A-I07 after 1 hour. Results shown here are representative of 3 independent experiments. (C) Wild-type B cells were stimulated with LPS (20 μg/mL) for 48 hours to allow the expression of XBP-1, and subsequently treated with DMSO (control), STF-083010 (50μM), A-I06 (50μM), or A-I07 (50μM) for 24 hours. Cells were lysed and analyzed for the expression of XBP-1, IRE-1, calreticulin, p97, and actin by immunoblots using specific Abs. Data shown in immunoblots are representative of 3 independent experiments. For each experiment, wild-type B cells were purified and pooled from 2 mouse spleens. (D) CLL cells isolated from 8-month-old Eμ-TCL1 mice were cultured in the presence of LPS. Simultaneously, these cells were treated with DMSO (control), STF-083010 (50μM), A-I06 (50μM), or A-I07 (50μM) for 48 hours. Cells were lysed and analyzed for the expression of XBP-1, p97, and actin by immunoblots using specific Abs. Data shown in immunoblots are representative of 3 independent experiments. For each experiment, CLL cells were purified and pooled from 2 Eμ-TCL1 mouse spleens. (E) CLL cells isolated from 8-month-old Eμ-TCL1 mice were cultured in the presence of LPS. Simultaneously, these cells were treated with DMSO (control), STF-083010 (50μM), A-I06 (50μM), or A-I07 (50μM) for 48 hours. Cells were lysed in TRIzol reagent to extract RNA. Unspliced and spliced forms of mouse XBP-1 mRNA, and mouse actin mRNA were detected by reverse transcription followed by PCR using specific primers. Results are representative of 3 independent experiments. For each experiment, CLL cells were purified and pooled from 2 Eμ-TCL1 mouse spleens. (F) WaC3 cells were treated with DMSO (control), STF-083010 (50 μM), A-I06 (50μM), or A-I07 (50μM) for 72 hours, and subsequently lysed for RNA extraction. Unspliced and spliced forms of human XBP-1 mRNA, and human actin mRNA were detected by reverse transcription followed by PCR using specific primers. Results are representative of 3 independent experiments. (G) Wild-type B cells were cultured in the presence of LPS and A-I06 (50μM) for indicated times and lysed for analysis by immunoblots using Abs against μ heavy chain, p97 and actin. Data shown in immunoblots are representative of 3 independent experiments. For each experiment, wild-type B cells were purified and pooled from 2 mouse spleens.

and MEC2 cells respond to STF-083010 or A-I06 with ~ 20% growth inhibition in the first 48 hours; however, these cells eventually overcome the inhibitory effect of each compound (Figure 7B-C). In contrast, WaC3 cells respond to treatments with STF-083010 or A-I06 with gradually decreased growth (Figure 7D). This can be explained by the fact that WaC3 cells have already acquired a constitutively phosphorylated IRE-1 (Figure 2D). We further treated MEC1 cells with A-I06 in combination with fludarabine, a Food and Drug Administration–approved purine analog for clinical CLL treatments. A-I06 synergizes with fludarabine to elicit

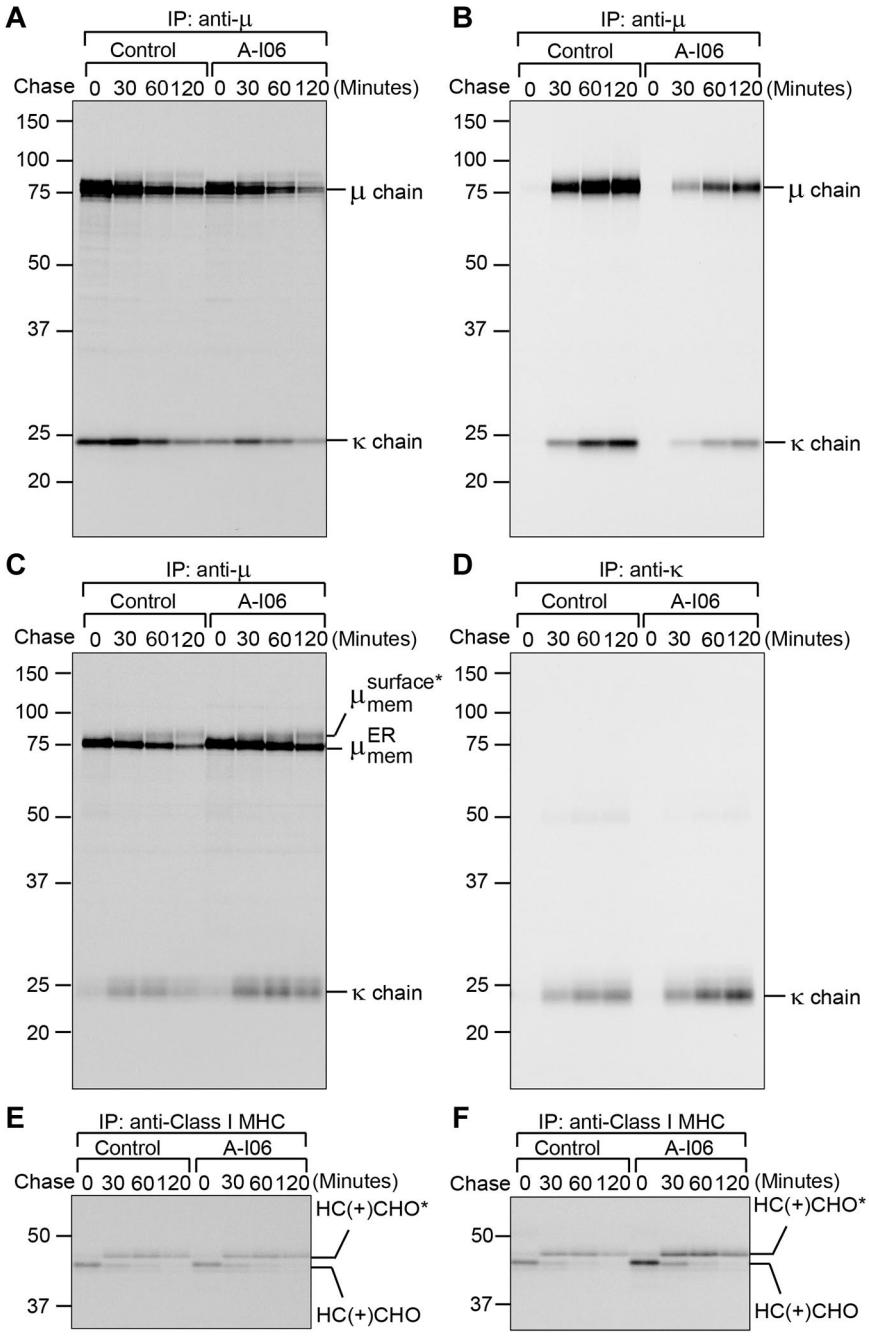

Figure 6. A-I06 inhibits the synthesis of secretory μ chains, but not membrane-bound μ chains, free κ chains, and membrane-bound class I MHC heavy chains (HC); A-I06 does not affect protein transport. (A-B) Wild-type B cells were stimulated with LPS for 2 days and subsequently treated with A-106 (50μM) for an additional day. Untreated control and A-I06–treated cells were radiolabeled for 15 minutes, chased for the indicated time, and lysed. Intracellular and extracellular IgM were immunoprecipitated from (A) lysates and (B) culture media, respectively, using an anti-μ Ab. Immunoprecipitates were analyzed on a SDS-PAGE gel. Data are representative of 2 independent experiments. For each experiment, wild-type B cells were purified and pooled from 2 mouse spleens. (C-D) To reveal the effect of A-I06 on mIgM, B cells purified from $\mu S^{-/-}$ mouse spleens were stimulated with LPS for 2 days and subsequently treated with A-I06 (50μM) for an additional day. Untreated control and A-I06–treated cells were radiolabeled for 15 minutes, chased for the indicated time, and lysed. (C) Intracellular mIgM was immunoprecipitated from lysates using an anti-μ Ab. (D) Secreted free κ chains were immunoprecipitated from culture media using an anti-κ Ab. Immunoprecipitates were analyzed on an SDS-PAGE gel. *Complex-type glycan modifications. Data are representative of 2 independent experiments. For each experiment, $\mu S^{-/-}$ B cells were purified and pooled from 2 mouse spleens. (E) Similar wild-type B-cell lysates as those in panel A were immunoprecipitated using an anti-class I MHC HC Ab and analyzed by SDS-PAGE. CHO and CHO* represent high mannose-type glycans and complex-type glycans, respectively. Data are representative of 2 independent experiments. For each experiment, wild-type B cells were purified and pooled from 2 mouse spleens. (F) Similar $\mu S^{-/-}$ B-cell lysates as those in panel C were immunoprecipitated using an anti–class I MHC HC Ab and analyzed by SDS-PAGE. Data are representative of 2 independent experiments. For each experiment, $\mu S^{-/-}$ B cells were purified and pooled from 2 mouse spleens.

a better growth inhibition effect on MEC1 cells (Figure 7E). Because primary human CLL cells expressed activated IRE-1 (Figure 2D, supplemental Figure 8A), we treated these cells with STF-083010, A-I06, or A-I07. STF-083010 and A-I06 exert a significant cytotoxic effect on primary human CLL cells by inducing apoptosis (Figure 7F-G, supplemental Figure 8B-J).

To test whether the IRE-1 inhibitor can inhibit CLL cell growth in mice, we injected CLL-bearing Eμ-TCL1 mice with A-I06, and observed reduced CLL burden during the course of treatment (Figure 7H). Such significant reduction in CLL burden can be explained by the increase of annexin V^+ apoptotic $CD5^+/B220^+$ CLL cells in A-I06–treated Eμ-TCL1 mice (Figure 7I-J right panels). Treatment with A-I06 does not induce $CD5^-/B220^+$ B cells to undergo apoptosis in Eμ-TCL1 CLL mice (Figure 7I-J middle panels).

Discussion

TCL1 is an oncoprotein contributing to the occurrence of T-cell prolymphocytic leukemia, as a result of chromosomal translocations and inversions at 14q31.2.[35] Although such a chromosomal defect is not found in CLL, TCL1 expresses in ~ 90% human CLL patients[22] (Figure 2D, supplemental Figure 8A). Significantly, TCL1 overexpression alone can drive the formation of mouse CLL.[21] Abnormal epigenetic regulations may account for abnormal expression of TCL1.[36] The oncogenic effect of TCL1 has been long believed to be a result of AKT activation. TCL1 physically binds to AKT, enhances the activity of AKT in phosphorylating glycogen synthase kinase-3, and promotes transport of AKT to the nucleus, contributing to cell survival and rapid proliferation.[28] Our new data

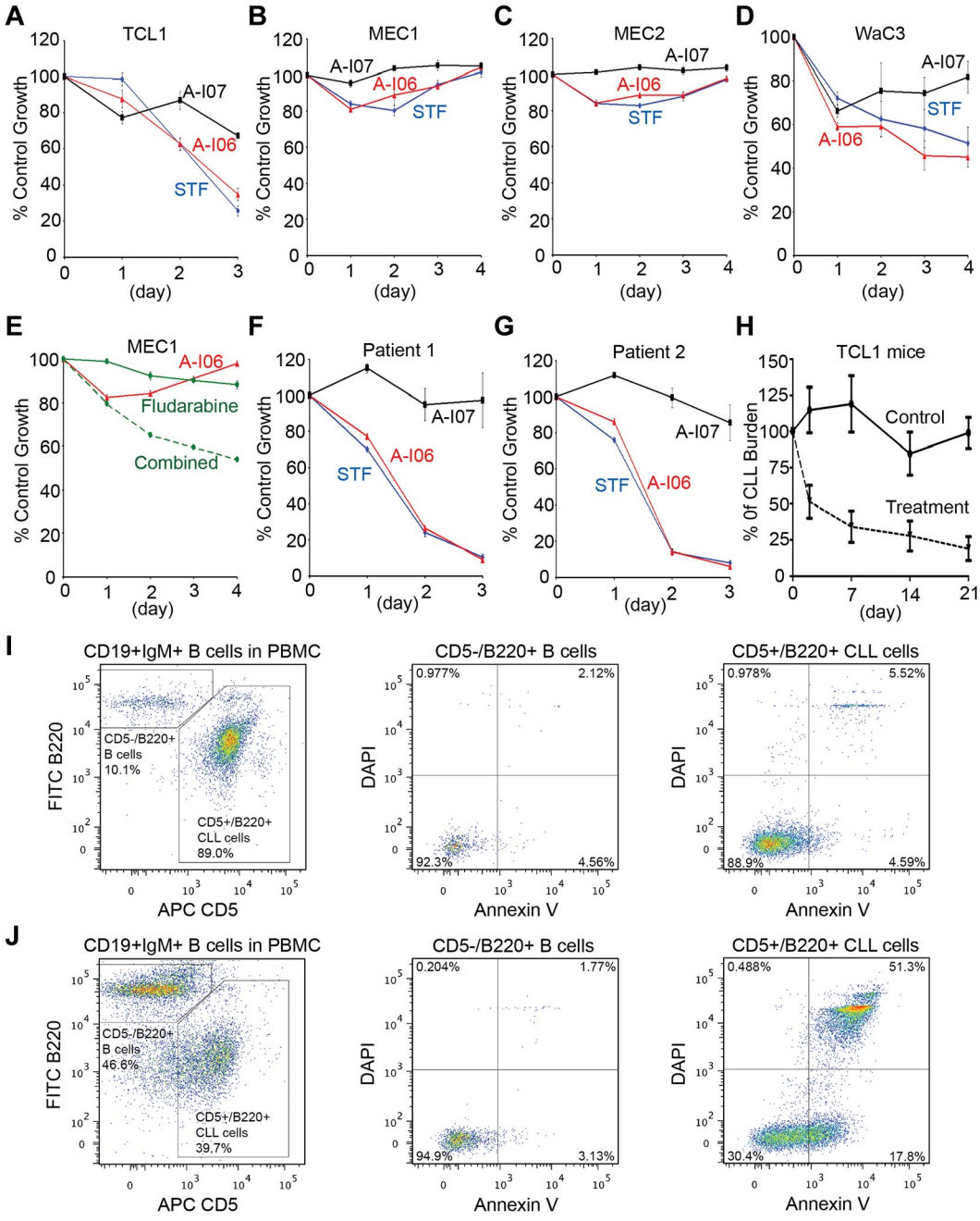

Figure 7. STF-083010 and its decomposed product, A-I06, stall growth of CLL cells by inducing apoptosis. (A) Eμ-TCL1 CLL cells, (B) MEC1 cells, (C) MEC2 cells, and (D) WaC3 cells were untreated or treated with STF-083010 (50μM), A-I06 (50μM), or A-I07 (50μM) for a course of 3 or 4 days, and subjected to XTT assays at the end of each day. Percentages of growth were determined by comparing treated with untreated groups. Each data point derived from 4 independent groups receiving exactly the same treatment was plotted as mean ± SD. (E) MEC1 cells were untreated or treated with A-I06 (50μM), fludarabine (30μM), or the combination of both for a course of 4 days, and subjected to XTT assays. Data derived from the same experimental settings were plotted as mean ± SD. (F-G) Primary human CLL cells isolated from patient 1 and patient 2 were untreated or treated with STF-083010 (50μM), A-I06 (50μM), or A-I07 (50μM) for a course of 3 days, and subjected to XTT assays. Data derived from the same experimental settings were plotted as mean ± SD. Results are representative of 3 independent experiments. (H) Eμ-TCL1 mice with high percentage of CLL cells in the peripheral blood were identified and injected intraperitoneally with vehicle (n = 9) or A-I06 (60 mg/kg; n = 5) on day 0, day 1, day 12 and day 13. The percentage of CLL cells in PBMCs for each mouse was determined by flow cytofluorometry on day 2, day 7, day 14, and day 21, and compared with the CLL burden data of the mouse on day 0 (100%). Data derived from multiple mice receiving exactly the same treatment were plotted as mean ± SEM. (I) PBMCs isolated from Eμ-TCL1 CLL mice injected with vehicle for 24 hours were stained with CD19-APC-Cy7, IgM–Alexa 568, CD5-APC, B220–Alexa 488, annexin V–PE, and DAPI. $CD5^-/B220^+$ B cells and $CD5^+/B220^+$ CLL cells were analyzed on gated $CD19^+/IgM^+$ B-cell populations (left panel). $CD5^-/B220^+$ B cells and $CD5^+/B220^+$ CLL cells were further gated, and analyzed for the presence of annexin V^+ and $DAPI^+$ populations (middle and right panels). Data are representative of 4 independent experiments. (J) PBMCs isolated from A-I06–injected Eμ-TCL1 CLL mice were stained with CD19-APC-Cy7, IgM–Alexa 568, CD5-APC, B220–Alexa 488, annexin V–PE and DAPI. $CD5^-/B220^+$ B cells and $CD5^+/B220^+$ CLL cells were analyzed on gated $CD19^+/IgM^+$ B-cell populations (left panel). $CD5^-/B220^+$ B cells and $CD5^+/B220^+$ CLL cells were further gated, and analyzed for the presence of annexin V^+ and $DAPI^+$ populations (middle and right panels). Data are representative of 4 independent experiments.

now reveal that TCL1 can contribute to activation of the ER stress response at the transcriptional level (Figure 2B, supplemental Figure 3), possibly through its association with the transcription factor, XBP-1 (Figure 2C). The dysregulated expression of XBP-1 may disrupt normal crosstalk between transcription factors (Figure 3), and promote constitutively active BCR signal transduction

(Figure 4A).[19] All of these data help to explain why a TCL1-overexpressed B cell can turn into CLL.

The functional roles of the ER stress-response proteins in CLL have been largely overlooked because CLL cells do not develop a prominent ER structure like the plasma cell cancer, multiple myeloma. In this study, we demonstrated that the ER stress response is critical for the growth of mouse and human CLL. Because CLL cells are genetically heterogeneous, they are difficult to treat. However, they may all share the ER stress response as their critical survival mechanism, which can be targeted for therapy. Geldanamycin and herbimycin A were used as inhibitors for GRP94 to induce apoptosis in CLL cells, and they synergized with fludarabine or chlorambucil in killing CLL cells.[11] Down-regulation of BiP by siRNA also induces apoptosis in CLL.[12] Although there is no precedent study on the expression of Derlin proteins in CLL cells (Figure 2B,D), Derlin-1 is overexpressed in many solid malignancies and is a potential molecular target for therapeutic intervention.[37] Our results now suggest that the IRE-1/XBP-1 pathway is a promising target for CLL treatment (Figure 7, supplemental Figure 8B-I). The inhibitor to the IRE-1/XBP-1 pathway, A-I06, induces apoptosis of mouse and human CLL cells in vitro (supplemental Figures 7, 8J) and selectively targets $CD5^+$ CLL cells in Eμ-TCL1 mice (Figure 7H-J).

TCL1 drives malignant progression of CLL via dysregulated expression of transcription factors and AID (Figure 3B). IRF4 alone can transform cells in vitro.[38] Although IRF4 is expressed in CLL, its contribution in patient survival outcome is unclear. Recent studies suggest a genetic variant of IRF4 common in CLL patients is associated with malignant progression of CLL.[39,40] IRF4 can up-regulate the expression of Blimp-1 by binding to the promoter region and fourth intron of the Blimp-1 gene, and directly regulate the expression of AID.[30,41,42] AID performs somatic hypermutation and class switch recombination in immunoglobulin genes. Such processes, if not confined to immunoglobulin genes, can contribute to the formation of cancer.[43] Increased expression of AID is indeed found in malignant CLL cases.[44,45]

TCL1 expression is associated with active BCR signal transduction,[23,24] which allows malignant CLL cells to sustain robust proliferation.[31] Targeting the BCR signaling pathway has been proposed as a therapeutic intervention for CLL.[46] In normal B cells, a functional BCR is composed of a mIgM and its associated disulfide-linked Igα/Igβ heterodimer. Both Igα and Igβ contain the immunoreceptor tyrosine-based activation motifs, whose phosphorylation leads to activation of a series of downstream signaling cascades. CLL cells use similar BCR signaling pathways.[31] We now show that TCL1 overexpression allows CLL cells to express a distinct BCR. Increased expression of mIgM and altered glycosylated Igα and Igβ (Figure 4B,E) may altogether contribute to the constitutively active BCR signal transduction in malignant CLL cells (Figure 4A).

Clinically, ~ 90% of CLL cases express TCL1.[22] When we examined the expression of TCL1 in CLL cells from 10 human patients, we found that TCL1 is not expressed in CLL cells from patient 10 (Figure 2D, supplemental Figure 8A). In addition, TCL1 is also not expressed in MEC1, MEC2, and WaC3 cells, which clearly exhibit the ER stress response (Figure 2D). While the role of TCL1 in activation of the ER stress response has been established using Eμ-TCL1 mice, the robust ER stress response found also in TCL1-null human CLL cells suggests that such activation can be achieved via other mechanisms. Interestingly, MEC1, MEC2, and WaC3 cells are all EBV-positive.[47,48] EBV can activate the ER stress response in B cells.[49]

Acknowledgments

The authors thank Dr Lori Hazlehurst for providing us with 5TGM1 cells, and Dr Jianguo Tao for useful discussions.

This work is partially supported by the Miles for Moffitt Foundation Funds (C.-C.A.H. and J.R.D.V.) and by Institutional Research Grant no. 93-032-16 from the American Cancer Society (C.-C.A.H.).

Authorship

Contribution: C.L.K., J.A.P.-I., A.W.M., J.J.P., C.-H.A.T., C.W.K., J.R.D.V., and C.-C.A.H. performed research; C.L.K., J.A.P.-I., A.W.M., C.-H.A.T., J.R.D.V., and C.-C.A.H. analyzed data; J.A.P.-I., J.J.P., N.Z., P.K.E.-B., E.M.S., and C.M.C. provided Eμ-TCL1 mice, human CLL cells, and useful suggestions to the research; and J.R.D.V. and C.-C.A.H. designed research and wrote the manuscript.

Conflict-of-interest disclosure: The authors declare no competing financial interests.

Correspondence: Chih-Chi Andrew Hu, PhD, or Juan R. Del Valle, PhD, Department of Immunology, H. Lee Moffitt Cancer Center, 12902 Magnolia Dr, Tampa, FL 33612; e-mail: chih-chi.hu@moffitt.org or juan.delvalle@moffitt.org.

References

1. Hamblin TJ, Davis Z, Gardiner A, Oscier DG, Stevenson FK. Unmutated Ig V(H) genes are associated with a more aggressive form of chronic lymphocytic leukemia. *Blood.* 1999;94(6):1848-1854.
2. Murray F, Darzentas N, Hadzidimitriou A, et al. Stereotyped patterns of somatic hypermutation in subsets of patients with chronic lymphocytic leukemia: implications for the role of antigen selection in leukemogenesis. *Blood.* 2008;111(3):1524-1533.
3. Widhopf GF 2nd, Goldberg CJ, Toy TL, et al. Nonstochastic pairing of immunoglobulin heavy and light chains expressed by chronic lymphocytic leukemia B cells is predicated on the heavy chain CDR3. *Blood.* 2008;111(6):3137-3144.
4. Chen L, Widhopf G, Huynh L, et al. Expression of ZAP-70 is associated with increased B-cell receptor signaling in chronic lymphocytic leukemia. *Blood.* 2002;100(13):4609-4614.
5. Lanham S, Hamblin T, Oscier D, Ibbotson R, Stevenson F, Packham G. Differential signaling via surface IgM is associated with VH gene mutational status and CD38 expression in chronic lymphocytic leukemia. *Blood.* 2003;101(3):1087-1093.
6. Chiron D, Bekeredjian-Ding I, Pellat-Deceunynck C, Bataille R, Jego G. Toll-like receptors: lessons to learn from normal and malignant human B cells. *Blood.* 2008;112(6):2205-2213.
7. Muzio M, Bertilaccio MT, Simonetti G, Frenquelli M, Caligaris-Cappio F. The role of toll-like receptors in chronic B-cell malignancies. *Leuk Lymphoma.* 2009;50(10):1573-1580.
8. Newell DG, Harris AH, Smith JL. The ultrastructural localization of immunoglobulin in chronic lymphocytic lymphoma cells: changes in light and heavy chain distribution induced by mitogen stimulation. *Blood.* 1983;61(3):511-519.
9. Carew JS, Nawrocki ST, Krupnik YV, et al. Targeting endoplasmic reticulum protein transport: a novel strategy to kill malignant B cells and overcome fludarabine resistance in CLL. *Blood.* 2006;107(1):222-231.
10. Rubartelli A, Sitia R, Zicca A, Grossi CE, Ferrarini M. Differentiation of chronic lymphocytic leukemia cells: correlation between the synthesis and secretion of immunoglobulins and the ultrastructure of the malignant cells. *Blood.* 1983;62(2):495-504.
11. Jones DT, Addison E, North JM, et al. Geldanamycin and herbimycin A induce apoptotic killing of B chronic lymphocytic leukemia cells and augment the cells' sensitivity to cytotoxic drugs. *Blood.* 2004;103(5):1855-1861.
12. Rosati E, Sabatini R, Rampino G, et al. Novel targets for endoplasmic reticulum stress-induced apoptosis in B-CLL. *Blood.* 2010;116(15):2713-2723.
13. Rutkowski DT, Hegde RS. Regulation of basal

cellular physiology by the homeostatic unfolded protein response. *J Cell Biol.* 2010;189(5):783-794.

14. Walter P, Ron D. The unfolded protein response: from stress pathway to homeostatic regulation. *Science.* 2011;334(6059):1081-1086.
15. Shen X, Ellis RE, Lee K, et al. Complementary signaling pathways regulate the unfolded protein response and are required for C. elegans development. *Cell.* 2001;107(7):893-903.
16. Yoshida H, Matsui T, Yamamoto A, Okada T, Mori K. XBP1 mRNA is induced by ATF6 and spliced by IRE1 in response to ER stress to produce a highly active transcription factor. *Cell.* 2001;107(7):881-891.
17. Calfon M, Zeng H, Urano F, et al. IRE1 couples endoplasmic reticulum load to secretory capacity by processing the XBP-1 mRNA. *Nature.* 2002; 415(6867):92-96.
18. Acosta-Alvear D, Zhou Y, Blais A, et al. XBP1 controls diverse cell type- and condition-specific transcriptional regulatory networks. *Mol Cell.* 2007;27(1):53-66.
19. Hu CC, Dougan SK, McGehee AM, Love JC, Ploegh HL. XBP-1 regulates signal transduction, transcription factors and bone marrow colonization in B cells. *EMBO J.* 2009;28(11):1624-1636.
20. Carrasco DR, Sukhdeo K, Protopopova M, et al. The differentiation and stress response factor XBP-1 drives multiple myeloma pathogenesis. *Cancer Cell.* 2007;11(4):349-360.
21. Bichi R, Shinton SA, Martin ES, et al. Human chronic lymphocytic leukemia modeled in mouse by targeted TCL1 expression. *Proc Natl Acad Sci U S A.* 2002;99(10):6955-6960.
22. Herling M, Patel KA, Khalili J, et al. TCL1 shows a regulated expression pattern in chronic lymphocytic leukemia that correlates with molecular subtypes and proliferative state. *Leukemia.* 2006; 20(2):280-285.
23. Herling M, Patel KA, Weit N, et al. High TCL1 levels are a marker of B-cell receptor pathway responsiveness and adverse outcome in chronic lymphocytic leukemia. *Blood.* 2009;114(21):4675-4686.
24. Holler C, Pinon JD, Denk U, et al. PKCbeta is essential for the development of chronic lymphocytic leukemia in the TCL1 transgenic mouse model: validation of PKCbeta as a therapeutic target in chronic lymphocytic leukemia. *Blood.* 2009;113(12):2791-2794.
25. Yan XJ, Albesiano E, Zanesi N, et al. B cell receptors in TCL1 transgenic mice resemble those of aggressive, treatment-resistant human chronic lymphocytic leukemia. *Proc Natl Acad Sci U S A.* 2006;103(31):11713-11718.
26. Johnson AJ, Lucas DM, Muthusamy N, et al. Characterization of the TCL-1 transgenic mouse as a preclinical drug development tool for human chronic lymphocytic leukemia. *Blood.* 2006; 108(4):1334-1338.
27. Boes M, Esau C, Fischer MB, Schmidt T, Carroll M, Chen J. Enhanced B-1 cell development, but impaired IgG antibody responses in mice deficient in secreted IgM. *J Immunol.* 1998; 160(10):4776-4787.
28. Pekarsky Y, Koval A, Hallas C, et al. Tcl1 enhances Akt kinase activity and mediates its nuclear translocation. *Proc Natl Acad Sci U S A.* 2000;97(7):3028-3033.
29. Teitell MA. The TCL1 family of oncoproteins: coactivators of transformation. *Nat Rev Cancer.* 2005;(8):640-648.
30. Klein U, Casola S, Cattoretti G, et al. Transcription factor IRF4 controls plasma cell differentiation and class-switch recombination. *Nat Immunol.* 2006;7(7):773-782.
31. Zenz T, Mertens D, Kuppers R, Dohner H, Stilgenbauer S. From pathogenesis to treatment of chronic lymphocytic leukaemia. *Nat Rev Cancer.* 2010;10(1):37-50.
32. McGehee AM, Dougan SK, Klemm EJ, et al. XBP-1-deficient plasmablasts show normal protein folding but altered glycosylation and lipid synthesis. *J Immunol.* 2009;183(6):3690-3699.
33. Papandreou I, Denko NC, Olson M, et al. Identification of an Ire1alpha endonuclease specific inhibitor with cytotoxic activity against human multiple myeloma. *Blood.* 2011;117(4):1311-1314.
34. Cross BC, Bond PJ, Sadowski PG, et al. The molecular basis for selective inhibition of unconventional mRNA splicing by an IRE1-binding small molecule. *Proc Natl Acad Sci U S A.* 2012; 109(15):E869-E878.
35. Virgilio L, Narducci MG, Isobe M, et al. Identification of the TCL1 gene involved in T-cell malignancies. *Proc Natl Acad Sci U S A.* 1994;91(26): 12530-12534.
36. Pekarsky Y, Santanam U, Cimmino A, et al. Tcl1 expression in chronic lymphocytic leukemia is regulated by miR-29 and miR-181. *Cancer Res.* 2006;66(24):11590-11593.
37. Ran Y, Hu H, Hu D, et al. Derlin-1 is overexpressed on the tumor cell surface and enables antibody-mediated tumor targeting therapy. *Clin Cancer Res.* 2008;14(20):6538-6545.
38. Iida S, Rao PH, Butler M, et al. Deregulation of MUM1/IRF4 by chromosomal translocation in multiple myeloma. *Nat Genet.* 1997;17(2):226-230.
39. Di Bernardo MC, Crowther-Swanepoel D, Broderick P, et al. A genome-wide association study identifies six susceptibility loci for chronic lymphocytic leukemia. *Nat Genet.* 2008;40(10): 1204-1210.
40. Allan JM, Sunter NJ, Bailey JR, et al. Variant IRF4/MUM1 associates with CD38 status and treatment-free survival in chronic lymphocytic leukaemia. *Leukemia.* 2010;24(4):877-881.
41. Sciammas R, Shaffer AL, Schatz JH, Zhao H, Staudt LM, Singh H. Graded expression of interferon regulatory factor-4 coordinates isotype switching with plasma cell differentiation. *Immunity.* 2006;25(2):225-236.
42. Shaffer AL, Emre NC, Lamy L, et al. IRF4 addiction in multiple myeloma. *Nature.* 2008; 454(7201):226-231.
43. Okazaki IM, Hiai H, Kakazu N, et al. Constitutive expression of AID leads to tumorigenesis. *J Exp Med.* 2003;197(9):1173-1181.
44. Albesiano E, Messmer BT, Damle RN, Allen SL, Rai KR, Chiorazzi N. Activation-induced cytidine deaminase in chronic lymphocytic leukemia B cells: expression as multiple forms in a dynamic, variably sized fraction of the clone. *Blood.* 2003;102(9):3333-3339.
45. McCarthy H, Wierda WG, Barron LL, et al. High expression of activation-induced cytidine deaminase (AID) and splice variants is a distinctive feature of poor-prognosis chronic lymphocytic leukemia. *Blood.* 2003;101(12):4903-4908.
46. Pleyer L, Egle A, Hartmann TN, Greil R. Molecular and cellular mechanisms of CLL: novel therapeutic approaches. *Nat Rev Clin Oncol.* 2009; 6(7):405-418.
47. Stacchini A, Aragno M, Vallario A, et al. MEC1 and MEC2: two new cell lines derived from B-chronic lymphocytic leukaemia in prolymphocytoid transformation. *Leuk Res.* 1999;23(2):127-136.
48. Wendel-Hansen V, Sallstrom J, De Campos-Lima PO, et al. Epstein-Barr virus (EBV) can immortalize B-cll cells activated by cytokines. *Leukemia.* 1994;8(3):476-484.
49. Lee DY, Sugden B. The LMP1 oncogene of EBV activates PERK and the unfolded protein response to drive its own synthesis. *Blood.* 2008; 111(4):2280-2289.